Light emission properties and mechanism of low-temperature prepared amorphous SiN_X films. II. Defect states electroluminescence

M. Wang,[1,2] J. Huang,[1] Z. Yuan,[1] A. Anopchenko,[2] D. Li,[1] D. Yang,[1,a)] and L. Pavesi[2]
[1]*State Key Laboratory of Silicon Materials, Department of Materials Science and Engineering, Zhejiang University, Hangzhou 310027, People's Republic of China*
[2]*Laboratorio Nanoscienze, Dipartimento di Fisica, Università di Trento, via Sommarive 14, 38100 Povo-Trento, Italy*

(Received 18 February 2008; accepted 23 August 2008; published online 21 October 2008)

In this paper, we present a room-temperature electroluminescence (EL) study of amorphous nonstoichiometric silicon nitride (SiN_X) films. The light-emitting device is formed by an ITO/SiN_X/*p*-type silicon structure. EL shows a yellowish broad emission spectrum with a power efficiency of 10^{-6}. The EL peak energy depends on the bias voltage rather than on the silicon content in SiN_X. By fitting the current-voltage characteristic with existing models, we found that under high voltages the Poole–Frenkel hole conduction is the main carrier transport mechanism in these devices. Injected electrons are captured by silicon dangling bonds (*K* center) and recombine with holes, which are localized in valence band tail states. Unbalanced hole and electron injection and nonradiative recombination are the main constraints on the EL efficiency of SiN_X. *© 2008 American Institute of Physics*. [DOI: 10.1063/1.2996299]

I. INTRODUCTION

The demand of cheap and complementary metal-oxide semiconductor (MOS) compatible light sources for optical interconnects[1,2] motivates the development of MOS light-emitting devices (MOS-LEDs), in which the gate insulator is incorporated with silicon nanocrystals or silicon nanocrystals coupled to rare-earth ions as the active component.[3–5] Silicon rich nitride (SiN_X) has been considered as one of the best candidate materials for this application since Park *et al.*[6] reported a tunable room-temperature photoluminescence (PL) and efficient electroluminescence (EL). Compared to silicon-rich oxide.[7] SiN_X has three main advantages: first of all, it has a lower barrier for carrier injection, especially for holes (the Si/Si_3N_4 band offset is smaller than Si/SiO_2 one); second, the possibility to achieve faster modulation than in silicon nanocrystals (much faster transitions are indicated by nanosecond luminescence lifetime of SiN_X);[8] and third, a lower processing temperature (high temperature annealing used to precipitate silicon nanocrystals in silicon-rich oxide is not necessary for SiN_X).[9,10]

Up to now, few EL investigations of SiN_X thin films have been reported,[11–14] where the light emission was usually observed in the visible range with a broad spectrum. Various EL mechanisms have been proposed. They are quantum confinement of silicon nanoclusters,[6] silicon-oxygen bonds,[14] and defect-related luminescence centers.[11]

The carrier transport in the metal-silicon nitride-silicon structure is of essential importance for the device performance. Because the Si/Si_3N_4 valence band offset (1.90 eV) is smaller than the conduction band offset (2.10 eV),[15] hole conduction is regarded as the main conducting mechanism[16] in silicon nitride. In addition, silicon dangling bonds form midgap states (*K* center), 3.1 eV above the valence band maxima, which are believed to act as an electron-capture center.[17]

In the previous paper, we showed that band tail states are involved in the PL of SiN_X. In this second paper, we investigate the EL and electrical characteristics of amorphous SiN_X films with three different compositions in an indium tin oxide (ITO)/SiN_X/*p*-type Si structure, where ITO acts as transparent contact. The origin of EL and its relation to carrier transport are discussed in an energy landscape, where midgap states are emphasized.

II. EXPERIMENTAL DETAILS

An ITO/SiN_X/*p*-type Si structure was realized for EL study. The substrate was a 5 μm 10–15 Ω cm boron doped *p*-type epitaxial layer on a heavily doped *p*-type (100) silicon wafer. 50 nm SiN_X films with three different compositions were deposited by plasma-enhanced chemical vapor deposition (CVD). The silicon content was adjusted by controlling the gas flow ratio of NH_3 to SiH_4, which was also used to label the sample (for example, N2 refers to a sample deposited with a ratio of NH_3 to SiH_4 equal to 2). Detailed parameters of the deposition can be found in our previous paper.[8]

An ITO electrode of 100 nm was sputtered on the SiN_X through a mask to define the device area. At the beginning, ITO and semitransparent gold electrodes have been tested. Similar spectra were obtained; however, since ITO is more transparent in the visible range, a higher EL intensity was observed from ITO devices. Therefore, in the following, the results obtained from ITO devices will be discussed.

A HF cleaning on the back of the substrate was carried out before forming the back contact. An Al layer of 300 nm

[a)]Author to whom correspondence should be addressed. Electronic mail: mseyang@zju.edu.cn. Tel.: +86-571-87951667. FAX: +86-571-87952322.

 © 2008 American Institute of Physics

Downloaded 27 Oct 2008 to 61.175.193.51. Redistribution subject to AIP license or copyright; see http://jap.aip.org/jap/copyright.jsp

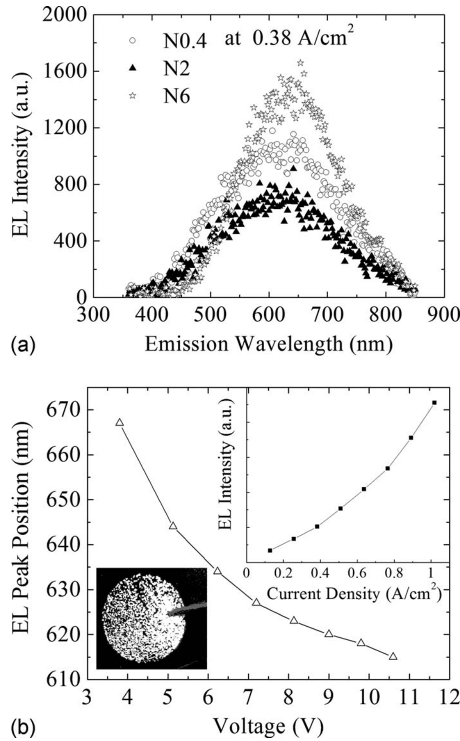

FIG. 1. EL properties of SiN_X films. (a) EL spectra from three samples with different compositions under the same injected current density ($0.38\ A/cm^2$). (b) Sample N6: EL emission wavelength vs applied voltage. Image of the emitting surface with a diameter of 10 mm (left inset). The integrated EL intensity vs injected current (right inset).

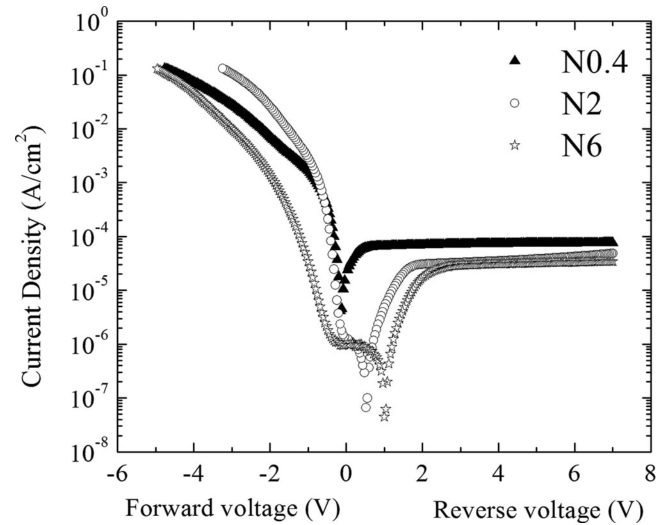

FIG. 2. Current density-voltage (J-V) characteristic of the devices with different active layers (N0.4, N2, and N6). The applied voltage was scanned from reverse to forward bias.

was evaporated on the back of the silicon substrate, followed by a rapid thermal annealing at 600 °C for 1 min in nitrogen to form an Ohmic contact.

The EL spectra of the devices driven by a dc power source were recorded in the visible range by an Acton SpectraPro-2500i monochromator coupled to a photomultiplier tube. Keithley 4200 SCS semiconductor parameter analyzer was used to measure the current-voltage characteristic of the devices. The total EL emitted power was collected by a large area *p-i-n* diode (UDT PIN-10DF), whose output current signal was measured by a Keithley 2400 sourcemeter. No corrections of geometrical factors on the reported data were applied.

III. RESULTS AND DISCUSSION

A. Electroluminescence

Figure 1(a) reports the EL spectra of SiN_X films with three different compositions at the same injection level ($0.38\ A/cm^2$). Although the PL spectra of these samples are located around red (N0.4), green (N2), and blue (N6) wavelengths,[8] the EL of all devices shows similar emission band at around 600 nm regardless of the composition. This suggests that states involved in the EL process might be different from those involved in the PL. The image of the emission pattern of N6 device driven at a current density of $0.7\ A/cm^2$ is shown in Fig. 1(b). Note that the emission area is composed by many shining spots, similar to the observation reported by Porjo *et al.*[18] in a Si/SiO_2 structure. They attributed those spots to some macroscopic structures between the active layer and the silicon substrate but not to microstructures such as silicon nanocrystals. In our case, these bright dots do not come from Joule heating because they can still be observed even under fairly low voltage such as 3.7 V ($0.13\ A/cm^2$). The density of the bright spots is smaller under low voltages and the emission wavelength is redshifted, as shown in Fig. 1(b). The integrated EL intensity is proportional to the injected current density and no saturation has been observed up to $1\ A/cm^2$.

B. Current-voltage characteristic and conduction mechanism

Current-voltage measurements were performed to understand the conduction mechanism of SiN_X. The substrate was grounded during the measurement. Applying a negative voltage on the ITO side is defined as forward bias, where substrate surface undergoes an accumulation of the majority carriers (holes, in this case). Figure 2 reports the current density-voltage (J-V) characteristics of samples N0.4, N2, and N6. The minimum of the J-V curve is positively shifted depending on the composition. The behaviors of N2 and N6 are quite similar; both of them have a minimum at positive voltage and show a plateau around 0 V, while no plateau was observed in N0.4 sample.

The minimum shift and the plateau suggest charging and discharging events inside the SiN_X. The voltage at the J-V curve minimum corresponds to the flat-band voltage of $ITO/SiN_X/p$-type Si structure. The flat-band voltage is given as $V_{FB}=\phi_{ms}-Q'_{ss}/C$,[19] where ϕ_{ms} is the work function difference between ITO and p-Si substrate (this in our case is close to zero),[20] Q'_{ss} is the charge inside the dielectric and C is the dielectric capacitance per unit area. Scanning the bias from reverse to forward, electrons are injected into the SiN_X layer from the silicon substrate and captured by trap states inside the SiN_X. These trap states are generally known as K center (silicon dangling bonds or $\equiv Si^0$). When capturing electrons, Q'_{ss} has a negative value, which causes a positive shift in the flat-band voltage. We also found that the mini-

Downloaded 27 Oct 2008 to 61.175.193.51. Redistribution subject to AIP license or copyright; see http://jap.aip.org/jap/copyright.jsp

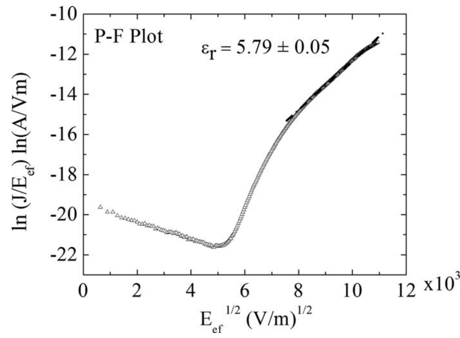

FIG. 3. Current density (J) vs the effective electrical field (E_{ef}) of device N6 plotted according to the PF model. The fitting was carried out in the high field region ($E_{ef} > 0.64$ MV/cm) where typical EL is observed. The dielectric constant (ε_r) of N6 was obtained from the fitting.

mum shifts farther in higher nitrogen content samples as well as wider plateau. As discussed in the previous paper,[8] more nitrogen in the SiN_X results in higher disorder and gap fluctuations, which create more localized states. This conclusion is consistent with the minimum shift in the J-V curves. When the curve goes into the left branch while the gate voltage is still a small positive value, the plateau can be found. At this moment, holes are injected from the substrate and neutralize the charged traps. The current increasing is limited by the recombination of holes with the trapped electrons. The higher is the density of trap states, the wider is the plateau.

To study the conduction mechanism[21] of the carriers in the SiN_X, the current density (J) versus effective electrical field (E_{ef}) data were fitted by Fowler–Nordheim (FN) tunneling[22] and Poole–Frenkel (PF) emission[23] models. The FN model is based on the hot electron tunneling through a triangle-shaped energy barrier formed in the dielectric layer due to the large applied electric field. The PF model describes the field enhanced thermal emission process of trapped electrons in the conduction band of the dielectric. The high voltage region of the forward bias J-E_{ef} curve was studied. Generally, a measurable EL signal starts to be detected under this region. Under this bias condition, the substrate undergoes an accumulation of holes so that the effective electric field can be roughly estimated by subtracting the flat-band voltage from the applied one, and then, dividing this value by the thickness of the active layer. Figure 3 shows the fitting of the N6 device curve by using the PF equation[23]

$$J_{PF} = CE_{ef} \exp[-q(\phi_B - \sqrt{qE_{ef}/\pi\varepsilon_r\varepsilon_0})/kT],$$

where q is elementary charge, ϕ_B is the energy barrier height for PF emission, ε_r is the relative static permittivity, ε_0 is the permittivity in free space, k is the Boltzmann constant, and T is the temperature. The parameters from the fitting can be helpful to check the validity of the model for this material. For example, by fitting the high voltage region of N6 curve (in this case $E_{ef} > 0.64$ MV/cm, equal to the applied voltage 4.2 V), the dielectric constant 5.79 ± 0.05 can be obtained. This value is slightly less than the constant of Si_3N_4 but between that of SiO_2 and Si_3N_4.[19] According to the refractive index and band gap, shown in the previous paper Table II,[8] the composition of N6 is close to Si_3N_4 but with a little oxygen content. This is consistent with the dielectric constant obtained from the modeling. The constants of all three samples are summarized in Table I. The values show the same trend as the refractive index[8] increases with the silicon content. N2, the silicon-rich sample,[8] can be considered as a mixture of amorphous silicon (11.7) and Si_3N_4 (7.5), so its dielectric constant is right between these values.[19] However, the constant of the highest silicon content sample (N0.4) is even larger than that of amorphous silicon. This indicates the departure of its conduction from the PF model. The FN model has also been used to examine this high voltage region. The band offset of silicon and SiN_X obtained from the FN model is almost one order of magnitude smaller than the theoretical value.[15] Therefore, we believe that PF emission dominates the carrier conduction in the voltage range where EL is observed.

TABLE I. Static dielectric constants (ε_r) of SiN_X with three different compositions extracted from fitting the experimental curves with the PF model. R is the regressive value for the fits.

Active layer	ε_r	R
N0.4	27.66 ± 0.34	0.996
N2	9.10 ± 0.15	0.996
N6	5.79 ± 0.05	0.999

C. Band structure and carrier transitions

The band structure of CVD deposited SiN_X has been widely discussed in the literature.[17,24] According to the work of Robertson and Powell,[17] Si–Si bonding states and $=N^-$ states generate 1.5 eV wide valence band tail, which is responsible for the PF hole conduction. On the other hand, silicon dangling bond defects, which act as electron traps, are located at 3.1 eV above the valence band maximum.[17] Based on these theoretical works and the current-voltage characteristics of our devices, the band gap structure, carrier transport, and recombination in the ITO/SiN_X/p-Si structure under forward bias are schematically drawn in Fig. 4. The holes are injected into the valence band tail, while the electrons are captured by the K center. The emitted photons energy should be equal to the energy difference between these holes and electrons, which is from 1.6 to 3.1 eV. The EL band around 2.0 eV is consistent with this estimation. Assuming that the silicon content has little influence on the energy difference between valence band tails and the K center,[17] the EL band will hardly be affected by the composition.

It is worth to emphasize that the power efficiency of our SiN_X LED is about 10^{-6}. Hole conduction by PF emission dominates the current at high voltage. In the meanwhile, electrons are injected from ITO into SiN_X assisted by defect states and then captured at the K center. In this sense the electron conduction is less favorable. If this is the case, we suspect that the population of injected holes is much larger than that of electrons. In addition, the electron barrier on the ITO side (about 2.5–3.3 eV, depending on the work function of ITO) (Ref. 20) is much higher than the hole barrier on the p-type silicon side, which is the Si/Si_3N_4 valence band offset (1.9 eV).[15] As a result, the injection of holes and electrons is unbalanced, so the probability of radiative recombination is

Downloaded 27 Oct 2008 to 61.175.193.51. Redistribution subject to AIP license or copyright; see http://jap.aip.org/jap/copyright.jsp

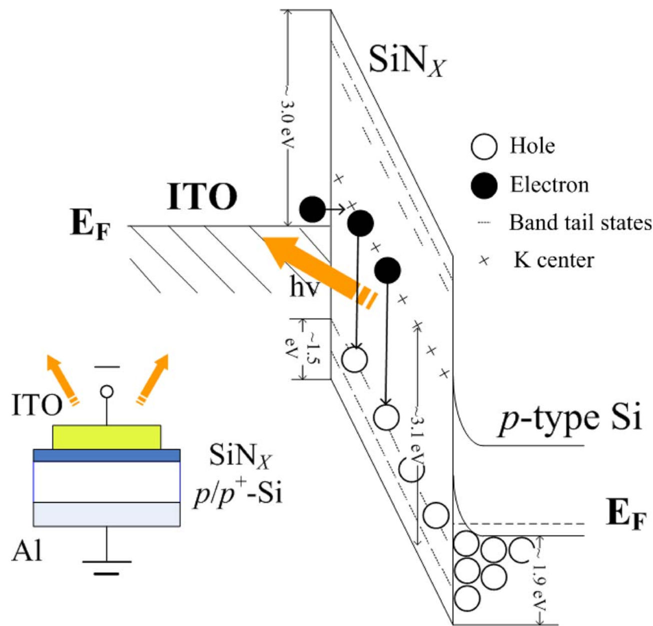

FIG. 4. (Color online) Schematic band diagram of ITO/SiN$_X$/*p*-type Si structure under forward bias. The device structure is also shown on the left.

low. Moreover, the strong nonradiative recombination also constrains the luminescence efficiency. In amorphous materials, nonradiative channels have been extensively discussed.[25,26] Most of them are attributed to the band tail and defect states originating from the structural disorder. Nonradiative and radiative processes probably both exist on these states, while the nonradiative one distinctly wins over the recombination process, resulting in both a lower EL efficiency and a faster PL decay.[8]

The reason of EL band blueshift by increasing the applied voltage is not so clear. One possible explanation could be that both injected holes and electrons can gain higher energy when a higher voltage is applied, which results in higher energy photons. Since the electron energy is fixed by the *K* center, the increasing voltage should affect more the energy of holes.

IV. CONCLUSIONS

Room-temperature EL of the ITO/SiN$_X$/*p*-type Si structure shows a broad emission spectrum with a yellowish color. The EL band, centered at about 620 nm, does not depend on the film composition. By studying the current-voltage characteristics, we conclude that PF hole conduction is the main carrier transport mechanism in SiN$_X$ under high voltage, where typical EL is observed. Electrons are injected through the midgap states formed by silicon dangling bonds. These electron-capture states leave distinct features in the *J-V* curves, which are explained by charging and discharging of traps. The EL power efficiency in these devices is about 10^{-6} because of the unbalanced injection of electrons and holes but mainly constrained by significant nonradiative processes. To conclude, the origin of the PL of SiN$_X$ is the band tail states, while most likely the EL can be assigned to the midgap electron-capture center in SiN$_X$.

ACKNOWLEDGMENTS

The work was financially supported by the National Natural Science Foundation of China (Grant No. 60606001), the PCSIRT Project, and 973 Project (Grant No. 2007CB613403). Valuable discussions with Dr. G. Pucker, Dr. M. Ghulinyan, and Dr. A. Picciotto at MT-Laboratory, FBK-IRST are gratefully acknowledged.

[1]M. Salib, L. Liao, R. Jones, M. Morse, A. Liu, D. Samara-Rubio, D. Alduino, and M. Paniccia, Intel Technol. J. **8**, 143 (2004).
[2]L. Pavesi and D. J. Lockwood, Top. Appl. Phys. **94**, 1 (2004).
[3]A. Irrera, F. Iacona, I. Crupi, C. D. Presti, G. Franzo, C. Bongiorno, D. Sanfilippo, G. Di Stefano, A. Piana, P. G. Fallica, A. Canino, and F. Priolo, Nanotechnology **17**, 1428 (2006).
[4]R. J. Walters, G. I. Bourianoff, and H. A. Atwater, Nature Mater. **4**, 143 (2005).
[5]M. E. Castagna, S. Coffa, M. Monaco, A. Muscara, L. Caristia, S. Lorenti, and A. Messina, Mater. Sci. Eng., B **105**, 83 (2003).
[6]N.-M. Park, T.-S. Kim, and S.-J. Park, Appl. Phys. Lett. **78**, 2575 (2001).
[7]F. Iacona, G. Franzo, and C. Spinella, J. Appl. Phys. **87**, 1295 (2000).
[8]M. Wang, M. Xie, L. Ferraioli, Z. Yuan, D. Li, D. Yang, and L. Pavesi, J. Appl. Phys. **104**, 083504 (2008).
[9]Y. Q. Wang, Y. G. Wang, L. Cao, and Z. X. Cao, Appl. Phys. Lett. **83**, 3474 (2003).
[10]T.-Y. Kim, N.-M. Park, K.-H. Kim, G. Y. Sung, Y.-W. Ok, and T.-Y. Seong, Appl. Phys. Lett. **85**, 5355 (2004).
[11]Z. Pei, Y. R. Chang, and H. L. Hwang, Appl. Phys. Lett. **80**, 2839 (2002).
[12]L.-Y. Chen, W.-H. Chen, and F. C.-N. Hong, Appl. Phys. Lett. **86**, 193506 (2005).
[13]B.-H. Kim, C.-H. Cho, S.-J. Park, N.-M. Park, and G. Y. Sung, Appl. Phys. Lett. **89**, 063509 (2006).
[14]R. Huang, K. Chen, H. Dong, D. Wang, H. Ding, W. Li, J. Xu, Z. Ma, and L. Xu, Appl. Phys. Lett. **91**, 111104 (2007).
[15]Y. C. Yeo, Q. Lu, W.-C. Lee, T.-J. King, and C. Hu, presented at the 58th Device Research Conference, Denver, CO, 2000 (unpublished), p. 65.
[16]A. J. Lowe, M. J. Powell, and S. R. Elliott, J. Appl. Phys. **59**, 1251 (1986).
[17]J. Robertson and M. J. Powell, Appl. Phys. Lett. **44**, 415 (1984).
[18]N. Porjo, T. Kuusela, and L. Heikkila, J. Appl. Phys. **89**, 4902 (2001).
[19]D. A. Neamen, *Semiconductor Physics and Devices: Basic Principles*, 3rd ed. (McGraw-Hill, New York, 2003).
[20]K. Sugiyama, H. Ishii, Y. Ouchi, and K. Seki, J. Appl. Phys. **87**, 295 (2000).
[21]B. L. Yang, P. T. Lai, and H. Wong, Microelectron. Reliab. **44**, 709 (2004).
[22]Z. A. Weinberg, J. Appl. Phys. **53**, 5052 (1982).
[23]S. M. Sze, J. Appl. Phys. **38**, 2951 (1967).
[24]R. Karcher, L. Ley, and R. L. Johnson, Phys. Rev. B **30**, 1896 (1984).
[25]R. A. Street, Phys. Rev. B **23**, 861 (1981).
[26]M. van der Voort, G. D. J. Smit, A. V. Akimov, and J. I. Dijkhuis, Physica B (Amsterdam) **263–264**, 283 (1999).

Downloaded 27 Oct 2008 to 61.175.193.51. Redistribution subject to AIP license or copyright; see http://jap.aip.org/jap/copyright.jsp